Journal of Photochemistry and Photobiology A: Chemistry 206 (2009) 220–226

Contents lists available at ScienceDirect

Journal of Photochemistry and Photobiology A: Chemistry

journal homepage: www.elsevier.com/locate/jphotochem

Fluorescence properties of a potential antitumoral benzothieno[3,2-*b*]pyrrole in solution and lipid membranes

Elisabete M.S. Castanheira[a,*], Ana S. Abreu[a,b], Maria-João R.P. Queiroz[b], Paula M.T. Ferreira[b], Paulo J.G. Coutinho[a], Nair Nazareth[c], M. São-José Nascimento[c]

[a] *Centro de Física, Universidade do Minho, Campus de Gualtar, 4710-057 Braga, Portugal*
[b] *Centro de Química, Universidade do Minho, Campus de Gualtar, 4710-057 Braga, Portugal*
[c] *Laboratório de Microbiologia, Centro de Estudos de Química Medicinal, da Universidade do Porto (CEQUIMED-UP), Faculdade de Farmácia, Rua Aníbal Cunha 164, 4050-047 Porto, Portugal*

ARTICLE INFO

Article history:
Received 10 March 2009
Received in revised form 30 June 2009
Accepted 3 July 2009

Keywords:
Benzothienopyrrole
Antitumour properties
Fluorescence
Lipid membranes

ABSTRACT

Fluorescence properties of the antitumoral methyl 3-(benzo[*b*]thien-2-yl)-benzothieno[3,2-*b*]pyrrole-2-carboxylate (**BTP**) were studied in solution and in lipid bilayers of dipalmitoyl phosphatidylcholine (DPPC), dioleoyl phosphatidylethanolamine (DOPE) and egg yolk phosphatidylcholine (Egg-PC). **BTP** presents good fluorescence quantum yields in all solvents studied ($0.20 \leq \Phi_F \leq 0.32$) and a bathochromic shift in polar solvents. The results indicate an ICT character of the excited state, with an estimated dipole moment of $\mu_e = 7.38$ D.

Fluorescence (steady-state) anisotropy measurements of **BTP** incorporated in lipid membranes of DPPC, DOPE and Egg-PC indicate that this compound is deeply located in the lipid bilayer, feeling the difference between the rigid gel phase and fluid phases.

BTP inhibits the growth of three human tumour cell lines, MCF-7 (breast adenocarcinoma), SF-268 (glioma) and NCI-H460 (non-small cell lung cancer), being significantly more potent against the NCI-H460 tumour cells.

1. Introduction

Thienopyrroles are a very important class of biologically active compounds with antiviral [1] and anti-inflammatory properties [2]. Thienopyrroles have been widely used as sPLA2 inhibitors [3], MCP-1 antagonists [4] and glycogen phosphorylase inhibitors [5]. This type of compounds has also been described as gonadotrophin releasing hormone antagonists [6] and as bioisosteric analogues of tryptamine derivatives [7].

Due to their broad spectrum of biological activity, strong research efforts have been devoted to the synthesis of thienopyrroles and their derivatives [8]. The skeleton benzothieno[3,2-*b*]pyrrole had already been synthesized by Iddon et al. [9] but, as far as our knowledge, no biological activity data have been reported on this type of compounds.

Recently, some of us have synthesized several fluorescent (benzo[*b*]thienyl)benzothienopyrroles [10]. One of these compounds, a methyl 3-(benzo[*b*]thien-2-yl)benzothieno[3,2-*b*]pyrrole-2-carboxylate (**BTP**) (Fig. 1) revealed promising antitumour properties, with a inhibitory activity of the in vitro growth of three human tumour cell lines, MCF-7 (breast adenocarcinoma), SF-268 (CNS cancer) and NCI-H460 (non-small cell lung cancer). The best anti-proliferative result was obtained for NCI-H460 cell line, with a very low GI_{50} value (concentration needed for 50% of cell growth inhibition) around 3.9 μM, as reported here.

These promising results suggested us to perform fluorescence studies of **BTP** incorporated in lipid membranes. The photophysical properties of **BTP** in solution and in lipid bilayers of neutral phospholipid components of biological membranes, DPPC (dipalmitoyl phosphatidylcholine), DOPE (dioleoyl phosphatidylethanolamine) and Egg-PC (egg yolk phosphatidylcholine) were studied. Fluorescence (steady-state) anisotropy measurements were also performed to obtain further information about the behaviour of **BTP** in lipid membranes. These studies are important, keeping in mind the incorporation of this compound in liposomes for controlled drug delivery systems. In fact, liposomes have been widely used to deliver anticancer agents, in order to reduce the

Abbreviations: DPPC, dipalmitoyl phosphatidylcholine; DOPE, dioleoyl phosphatidylethanolamine; Egg-PC, egg yolk phosphatidylcholine; PC, phosphatidylcholine; PE, phosphatidylethanolamine.

* Corresponding author. Tel.: +351 253 604321; fax: +351 253 604061.
E-mail addresses: ecoutinho@fisica.uminho.pt, emsccoutinho@gmail.com (E.M.S. Castanheira).

1010-6030/$ – see front matter © 2009 Elsevier B.V. All rights reserved.
doi:10.1016/j.jphotochem.2009.07.007

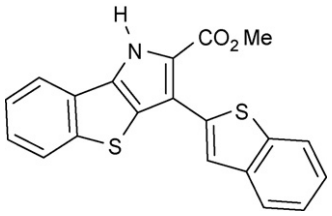

Fig. 1. Structure of the benzothieno[3,2-*b*]pyrrole (**BTP**) studied.

toxic effects of the drugs when given alone or to increase the drug circulation time and effectiveness [11].

2. Experimental

2.1. Materials and methods

All the solutions were prepared using spectroscopic grade solvents and ultrapure water (Milli-Q grade). 1,2-Dipalmitoyl-*sn*-glycero-3-phosphocholine (DPPC), 1,2-dioleoyl-*sn*-glycero-3-phosphoethanolamine (DOPE), and 1,2-diacyl-*sn*-glycero-3-phosphocholine from egg yolk (Egg-PC) were obtained from Sigma–Aldrich (lipid structures are shown below).

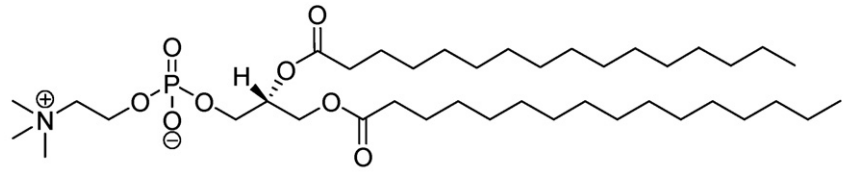

DPPC

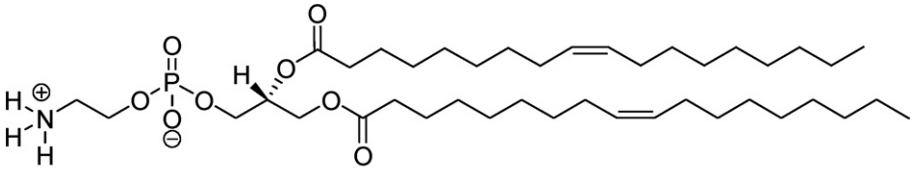

DOPE

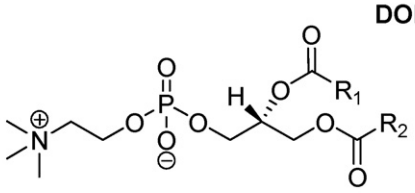

Egg-PC

For DOPE and Egg-PC membranes preparation, defined volumes of stock solutions of lipid (26.9 mM for DOPE and 34.5 mM for Egg-PC) and **BTP** (0.2 mM) in ethanol were injected together, under vigorous stirring, to an aqueous buffer solution (10 mM Tris, 1 mM EDTA, pH 7.4), at room temperature. A similar procedure was adopted for DPPC vesicles, but the injection of the required amounts of stock solutions of lipid (50 mM) and **BTP** in ethanol was done at 60 °C, well above the melting transition temperature of DPPC (*ca.* 41 °C) [12]. In all cases, the final lipid concentration was 1 mM, with a **BTP**/lipid molar ratio of 1:500.

2.2. Spectroscopic measurements

Absorption spectra were recorded in a Shimadzu UV-3101PC UV-Vis-NIR spectrophotometer. Fluorescence measurements were performed using a Fluorolog 3 spectrofluorimeter, equipped with double monochromators in both excitation and emission, Glan–Thompson polarizers and a temperature controlled cuvette holder. Fluorescence spectra were corrected for the instrumental response of the system.

For fluorescence quantum yield determination, the solutions were previously bubbled for 20 min with ultrapure nitrogen. The fluorescence quantum yields (Φ_s) were determined using the standard method (Eq. (1)) [13,14]. 9,10-Diphenylanthracene in ethanol was used as reference, $\Phi_r = 0.95$ [15]:

$$\Phi_s = \left[\frac{A_r F_s n_s^2}{A_s F_r n_r^2}\right] \Phi_r \quad (1)$$

where A is the absorbance at the excitation wavelength, F the integrated emission area and n the refraction index of the solvents used. Subscripts refer to the reference (r) or sample (s) compound. The absorbance value at excitation wavelength was always less than 0.1, in order to avoid inner filter effects.

Solvatochromic shifts were described by the Lippert–Mataga equation (2), which relates the energy difference between absorption and emission maxima to the orientation polarizability [16,17]:

$$\bar{\nu}_{abs} - \bar{\nu}_{fl} = \frac{1}{4\pi\varepsilon_0}\frac{2\Delta\mu^2}{hcR^3}\Delta f + \text{const} \quad (2)$$

where $\bar{\nu}_{abs}$ is the wave number of maximum absorption, $\bar{\nu}_{fl}$ is the wave number of maximum emission, $\Delta\mu = \mu_e - \mu_g$ is the difference in the dipole moment of solute molecule between excited (μ_e) and ground (μ_g) states, R is the cavity radius (considering the fluorophore a point dipole at the center of a spherical cavity immersed in the homogeneous solvent), and Δf is the orientation polarizability given by (Eq. (3)):

$$\Delta f = \frac{\varepsilon - 1}{2\varepsilon + 1} - \frac{n^2 - 1}{2n^2 + 1} \quad (3)$$

where ε is the static dielectric constant and n the refractive index of the solvent.

The steady-state fluorescence anisotropy, r, is calculated by:

$$r = \frac{I_{VV} - GI_{VH}}{I_{VV} + 2GI_{VH}} \quad (4)$$

where I_{VV} and I_{VH} are the intensities of the emission spectra obtained with vertical and horizontal polarization, respectively

(for vertically polarized excitation light), and $G = I_{HV}/I_{HH}$ is the instrument correction factor, where I_{HV} and I_{HH} are the emission intensities obtained with vertical and horizontal polarization (for horizontally polarized excitation light).

2.3. Biological activity

2.3.1. Materials

Fetal bovine serum (FBS) and L-glutamine were obtained from Gibco Invitrogen Co. (Scotland, UK). RPMI-1640 medium was from Cambrex (New Jersey, USA). Dimethylsulfoxide (DMSO), doxorubicin, penicillin, streptomycin and sulforhodamine B (SRB) were from Sigma Chemical Co. (Saint Louis, USA).

Stock solution of **BTP** was prepared in DMSO and kept at −20 °C. Appropriate dilutions of the compound were freshly prepared just prior to the assays. Final concentrations of DMSO did not interfere with the cell lines growth.

2.3.2. Cell cultures

Three human tumour cell lines, MCF-7 (breast adenocarcinoma), SF-268 (glioma) and NCI-H460 (non-small cell lung cancer) were used. MCF-7 was obtained from the European Collection of Cell Cultures (ECACC, Salisbury, UK). SF-268 and NCI-H460 were kindly provided by the National Cancer Institute (NCI, Bethesda, USA). Cells were grown as monolayer and routinely maintained in RPMI-1640 medium supplemented with 5% heat inactivated FBS, 2 mM glutamine and antibiotics (penicillin 100 U/ml and streptomycin 100 μg/ml), at 37 °C in a humidified atmosphere containing 5% CO_2. Exponentially growing cells were obtained by plating 1.5×10^5 cells/ml for MCF-7 and SF-268 and 0.75×10^5 cells/ml for NCI-H460, followed by 24 h incubation. The effect of the vehicle solvent (DMSO) on the growth of these cell lines was evaluated in all the experiments by exposing untreated control cells to the maximum concentration (0.5%) of DMSO used in each assay.

2.3.3. Tumour cells growth assay

The effect of **BTP** on the in vitro growth of human tumour cell lines was evaluated according to the procedure adopted by the National Cancer Institute (NCI, USA) in the "In vitro Anticancer Drug Discovery Screen" that uses the protein-binding dye sulforhodamine B to assess cell growth [18–19]. Briefly, exponentially cells growing in 96-well plates were exposed for 48 h to five serial concentrations of **BTP**, starting from a maximum concentration of 150 μM. Following this exposure period, adherent cells were fixed, washed and stained. The bound stain was solubilized and the absorbance was measured at 492 nm in a plate reader (BioTek Instruments Inc., Powerwave XS, Winooski, USA). A dose–response curve was obtained and the growth inhibition of 50% (GI_{50}), corresponding to the concentration of **BTP** that inhibited 50% of the net cell growth was calculated as described elsewhere [19]. Doxorubicin used as a positive control was tested in the same manner.

3. Results and discussion

3.1. Antitumoral properties of *BTP*

The effect of the benzothienopyrrole **BTP** on the in vitro growth of three human tumour cell lines, MCF-7 (breast adenocarcinoma), SF-268 (CNS cancer) and NCI-H460 (non-small cell lung cancer), was evaluated after a continuous exposure of 48 h. Results given in concentrations that were able to cause 50% of cell growth inhibition (GI_{50}) are summarized in Table 1.

It can be observed in Table 1 that **BTP** inhibited the growth of all the three human tumour cell lines, but it was significantly much more potent against the lung cancer NCI-H460 cell line, presenting a very low GI_{50} value (3.9 ± 0.3 μM). **BTP** presents GI_{50} values lower or of the same magnitude of other compounds recently tested in the same tumour cell lines and also considered as potential antitumorals [20,21]. The **BTP** different cell line response may reflect a possible tumour type-specific sensitivity of this compound which is very important for its potential use in the treatment of this type of tumour.

Table 1
Values of **BTP** concentration needed for 50% of cell growth inhibition (GI_{50}) for three human tumour cell lines.

Cell line	GI_{50} (μM)
MCF-7	19.1 ± 11.5
SF-268	38.7 ± 8.9
NCI-H460	3.9 ± 0.3

Results represent means ± SEM of 3–4 independent experiments performed in duplicate. Doxorubicin was used as positive control, GI_{50}: MCF-7 = 42.8 ± 8.2 nM; SF-268 = 94.0 ± 7.0 nM and NCI-H460 = 94.0 ± 8.7 nM.

Doxorubicin, used as positive control, presents a very high cytotoxicity because the planar aromatic part efficiently intercalates into DNA base pairs, while the six-membered daunosamine sugar binds to the minor groove, interacting with flanking base pairs adjacent to the intercalation site [22]. Nevertheless, doxorubicin presents also a high toxicity for the human body and the search for other antitumour compounds even less active but also less toxic is still an active domain of interest.

3.2. Photophysical properties of *BTP* in solution

The absorption and fluorescence properties of **BTP** were first studied in several solvents. The maximum absorption (λ_{abs}) and emission (λ_{em}) wavelengths, molar extinction coefficients and fluorescence quantum yields are presented in Table 2.

In pyrrole and its derivatives, the heteronitrogen is singly bonded to carbon atoms in the heterocycle. The transitions involving the non-bonding electrons have properties similar to those of $\pi \rightarrow \pi^*$ transitions, as the non-bonding orbital is perpendicular to the plane of the ring, which allows it to overlap the π orbitals on the adjacent carbon atoms [23]. **BTP** compound also presents a carboxylate group and it is known that many carbonyl compounds exhibit low fluorescence quantum yields due to the low-lying $n \rightarrow \pi^*$ state. In **BTP**, it is possible that the electronic transitions $\pi \rightarrow \pi^*$ and $n \rightarrow \pi^*$ can be nearby in energy, resulting in state-mixing [24]. A predominance of $\pi \rightarrow \pi^*$ character could explain the high ε values ($\varepsilon > 10^4\ M^{-1}\ cm^{-1}$) and the very reasonable fluorescence quantum yields (Table 2).

The normalized fluorescence spectra of **BTP** are shown in Fig. 2. Examples of absorption spectra are shown as inset.

A red shift can be observed from cyclohexane to more polar solvents, especially in fluorescence spectra. A complete loss of vibrational structure is also observed for the emission in polar solvents (Fig. 2), which is usually related to an intramolecular charge transfer (ICT) mechanism and/or to specific solvent effects [16]. This behaviour was already observed by us for tetracyclic benzothiophene derivatives, a thieno-δ-carboline and a methoxylated benzothieno[2,3-*c*]quinolone, synthesized by our group [25,26].

The Lippert–Mataga plot (Eq. (2)) for **BTP**, shown in Fig. 3, is reasonably linear in non-protic solvents, alcohols and chloroform exhibiting large positive deviations.

This behaviour in alcohols and chloroform can be attributed to specific solute–solvent interactions by hydrogen bonds. The formation of hydrogen bonds between chloroform and proton acceptors is known since a long time [28]. In fact, **BTP** has the capability of hydrogen bonding formation through the ester group

Table 2
Maximum absorption (λ_{abs}) and emission wavelengths (λ_{em}), molar extinction coefficients (ε) and fluorescence quantum yields (Φ_F) for **BTP** in several solvents.

Solvent	λ_{abs} (nm) (ε (M^{-1} cm^{-1}))	λ_{em} (nm)	Φ_F[a]
Cyclohexane	320 sh (2.33×10^4) 294 (3.30×10^4) 264 (3.10×10^4) 230 (3.26×10^4)	396	0.31
Dioxane	321 sh (2.59×10^4) 297 (3.81×10^4) 263 (3.36×10^4) 228 (4.15×10^4)	398	0.29
Diethyl ether	322 sh (1.67×10^4) 294 (2.46×10^4) 263 (2.03×10^4) 231 (1.92×10^4)	396	0.20
Ethyl acetate	324 sh (1.67×10^4) 295 (2.57×10^4)[b]	399	0.32
Dichloromethane	326 sh (2.62×10^4) 296 (3.79×10^4) 265 (3.36×10^4) 226 (4.35×10^4)	401	0.27
Chloroform	328 sh (1.70×10^4) 297 (2.30×10^4) 266 (2.10×10^4)[b]	406	0.30
Acetonitrile	326 sh (2.24×10^4) 294 (3.50×10^4) 262 (2.94×10^4) 228 (3.54×10^4)	399	0.23
N,*N*-Dimethylformamide	328 sh (3.09×10^4) 297 (4.86×10^4)[b]	402	0.29
Dimethylsulfoxide	331 sh (3.20×10^4) 299 (5.04×10^4)[b]	406	0.29
Ethanol	327 sh (2.73×10^4) 295 (4.24×10^4) 264 (3.50×10^4) 229 (4.03×10^4)	407	0.20
Methanol	328 sh (2.91×10^4) 294 (4.47×10^4) 263 (3.76×10^4) 228 (4.36×10^4)	411	0.20

sh, shoulder.
[a] Relative to 9,10-diphenylanthracene in ethanol ($\Phi_r = 0.95$ [15]). Error about 10%.
[b] *Solvents cut-off*: chloroform, 250 nm; ethyl acetate, 265 nm; dimethylsulfoxide, 270 nm; *N*,*N*-dimethylformamide, 275 nm.

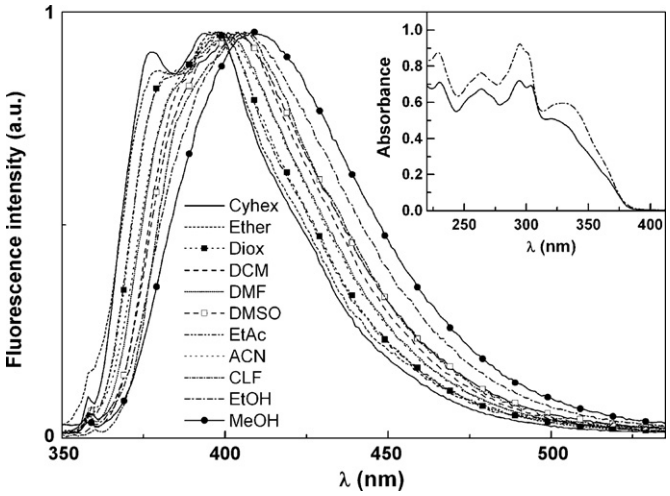

Fig. 2. Normalized fluorescence spectra (at peak of maximum emission) of 3×10^{-6} M solutions of **BTP** in several solvents ($\lambda_{exc} = 325$ nm) (Cyhex, cyclohexane; Ether, diethyl ether; Diox, dioxane; DCM, dichloromethane; DMF, *N*,*N*-dimethylformamide; DMSO, dimethylsulfoxide; EtAc, ethyl acetate; ACN, acetonitrile; CLF, chloroform; EtOH, ethanol; MeOH, methanol). Inset: absorption spectra of 2×10^{-5} M solutions of **BTP** in cyclohexane and ethanol, as examples (cell path = 1.0 cm).

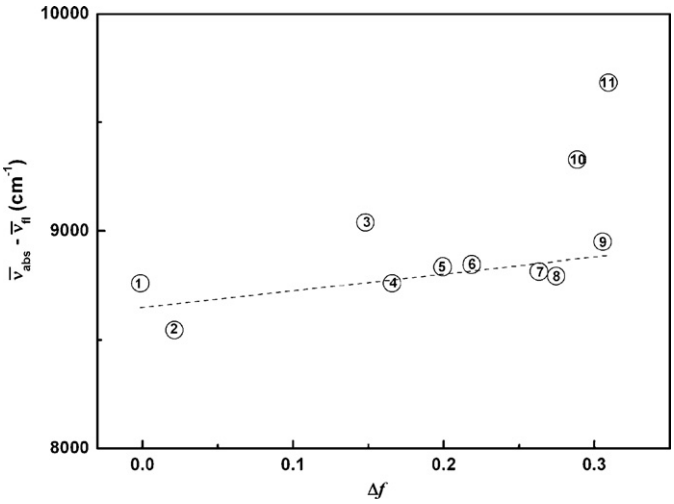

Fig. 3. Lippert–Mataga plot for **BTP**: (1) cyclohexane; (2) dioxane; (3) chloroform; (4) diethyl ether; (5) ethyl acetate; (6) dichloromethane; (7) dimethylsulfoxide; (8) *N*,*N*-dimethylformamide; (9) acetonitrile; (10) ethanol; (11) methanol (values of ε and n were obtained from Ref. [27]).

(acceptor), the two S atoms (acceptors) and also the pyrrolic NH group (donor).

From *ab initio* molecular quantum chemistry calculations, the cavity radius (R) and ground state dipole moment (μ_g) were determined, through an optimized structure provided by GAMESS software [29], using a RHF/3-21G(d) basis set [30] (Fig. 4). The **BTP** optimized geometry shows that the benzo[*b*]thienyl substituent of the molecule is almost perpendicular to the benzothienopyrrole system. A cavity radius of 7.9 Å and a ground state dipole moment of 1.24 D were obtained, allowing the estimation of an excited-state dipole moment of $\mu_e = 7.38$ D from the Lippert–Mataga plot. This μ_e value points to the presence of an intramolecular charge transfer (ICT) mechanism occurring in the planar benzothienopyrrole moiety, although not very pronounced. Twisted intramolecular charge transfer states (TICT) usually exhibit significantly higher excited-state dipole moments ($\geq$20 D) [31] than the value obtained for **BTP**.

Fig. 5 reports the representation of **BTP** HOMO and LUMO molecular orbitals. It can be observed that both molecular orbitals are localized on the benzothienopyrrole moiety and also on the methylester group. The HOMO–LUMO transition exhibits a charge transfer from the S atom of the benzothienopyrrole system to both

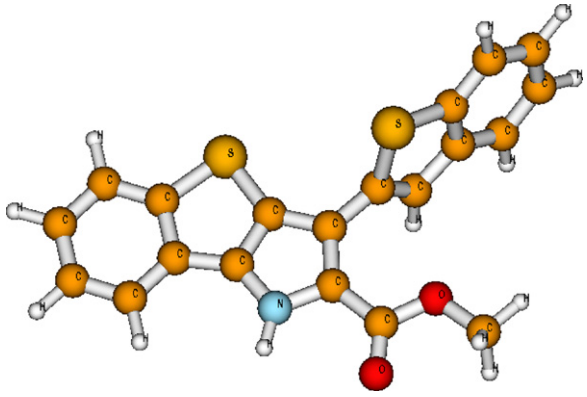

Fig. 4. Optimized structure of **BTP** (obtained by GAMESS software).

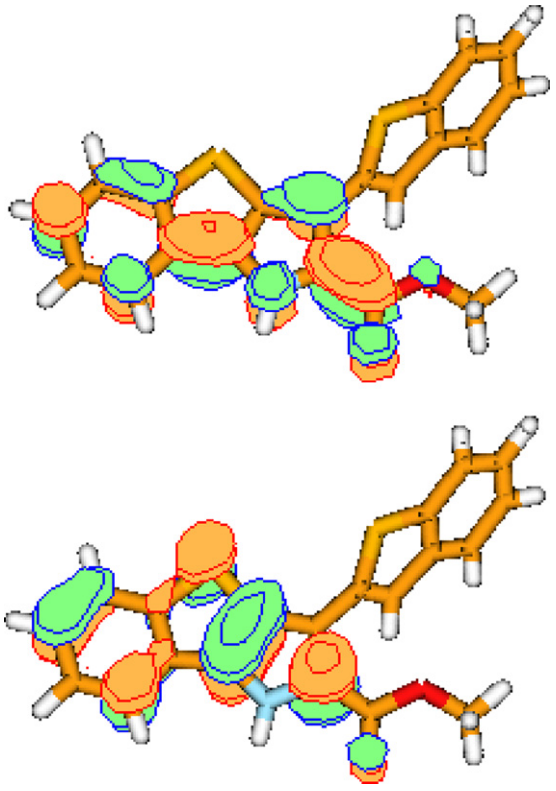

Fig. 5. Representation of HOMO (lower) and LUMO (upper) molecular orbitals of **BTP**.

the nitrogen and the OMe oxygen, confirming the ICT character of the excited state.

The benzo[*b*]thienyl substituent does not contribute to increase non-radiative deactivation pathways in **BTP**. This justifies the reasonable fluorescence quantum yields obtained (between 20% and 32%, Table 2), despite the presence of two S atoms in the molecule, which usually lead to the increase of singlet–triplet intersystem crossing by enhancement of spin–orbit coupling interaction [24]. The contribution of S atoms to decrease the fluorescence quantum yield is less important for **BTP** than for other analogues like benzothienoindoles with a dibenzothienyl substituent already synthesized and studied by us [32].

3.3. Interaction of *BTP* with lipid membranes

Due to its promising antitumoral activity, photophysical studies of **BTP** incorporated in lipid bilayers were also performed. These studies are relevant to evaluate the interaction of the compound with lipid membranes. Assessment of the localization of **BTP** in lipid vesicles is also important, pointing to drug delivery applications using liposomes.

Different types of phospholipid molecules, DPPC, Egg-PC and DOPE, were used for vesicle preparation. At room temperature, DPPC (16:0 PC) is in the ordered gel phase, where the hydrocarbon chains are fully extended and closely packed. Above the melting transition temperature, T_m = 41 °C [12], DPPC attains the disordered liquid-crystalline phase. DOPE (18:1 PE) exhibits a very low melting transition temperature (T_m = −16 °C [33]) and presents a lamellar bilayer to inverse hexagonal (L_α–H_{II}) phase transition at 3.3 °C [34]. Egg-PC is a natural phospholipid mixture, where molecules have the same polar head group (phosphatidylcholine) and different hydrocarbon chains, differing in length and degree of unsaturation. Main components are 16:0 PC, 18:0 PC and 18:1 PC [35]. Therefore, at room temperature, Egg-PC is in the fluid liquid-crystalline phase.

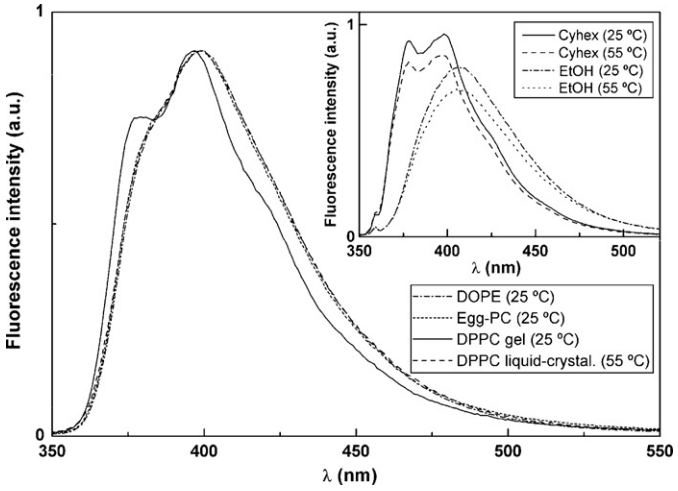

Fig. 6. Normalized fluorescence spectra of **BTP** in lipid membranes of DOPE, Egg-PC and DPPC (λ_{exc} = 325 nm). Inset: fluorescence spectra of **BTP** in cyclohexane (Cyhex) and ethanol (EtOH), at 25 and 55 °C.

In DPPC vesicles at gel phase (25 °C), the emission spectrum of **BTP** is very similar in shape and position to those in cyclohexane and diethyl ether (Fig. 6 and Table 3), indicating that **BTP** is located deeply inside the lipid bilayer. When DPPC is in the liquid-crystalline phase (at 55 °C), a structureless and red-shifted emission is observed, similar to the spectra obtained in dioxane and ethyl acetate. A decrease in emission intensity of about 25% is also detected.

In homogeneous solution, the effect of increasing temperature in the fluorescence of **BTP** is a 10% intensity reduction and a very small blue shift (*ca.* 1 nm). The inset of Fig. 6 shows **BTP** emission spectra in cyclohexane and ethanol at 25 and 55 °C, where it can be seen that the spectral shape is roughly the same at both temperatures.

The red shift and loss of vibrational structure of **BTP** emission in lipid membranes at fluid phases (DOPE and Egg-PC at 25 °C and DPPC at 55 °C) point to a higher penetration of water molecules in the vesicle bilayer, as lipid hydrocarbon chains are randomly oriented and fluid. However, it is also possible that in fluid phases **BTP** locates in a more polar environment, near the ester groups of the phospholipid molecules.

Fluorescence anisotropy measurements can give further information about **BTP** behaviour in lipid membranes. Steady-state anisotropy relates to both the excited-state lifetime and the rotational correlation time of the fluorophore [23]:

$$\frac{1}{r} = \frac{1}{r_0}\left(1 + \frac{\tau}{\tau_c}\right) \quad (5)$$

where r_0 is the fundamental anisotropy, τ is the excited-state lifetime and τ_c is the rotational correlation time.

The fluorescence steady-state anisotropies and fluorescence quantum yields of **BTP** in lipid bilayers are shown in Table 3.

Table 3
Steady-state fluorescence anisotropy (r) values, fluorescence quantum yields and maximum emission wavelengths (λ_{em}) of **BTP** in lipid membranes. Values in ethylene glycol at room temperature are also shown for comparison.

	λ_{em} (nm)	Φ_F[a]	r
Egg-PC (25 °C)	400	0.24	0.046
DOPE (25 °C)	399	0.27	0.023
DPPC (25 °C)	397	0.26	0.058
DPPC (55 °C)	399	0.11	0.036
Ethylene glycol (25 °C)	415	0.29	0.036

[a] Relative to 9,10-diphenylanthracene in ethanol (Φ_r = 0.95 [15]). Error about 10%.

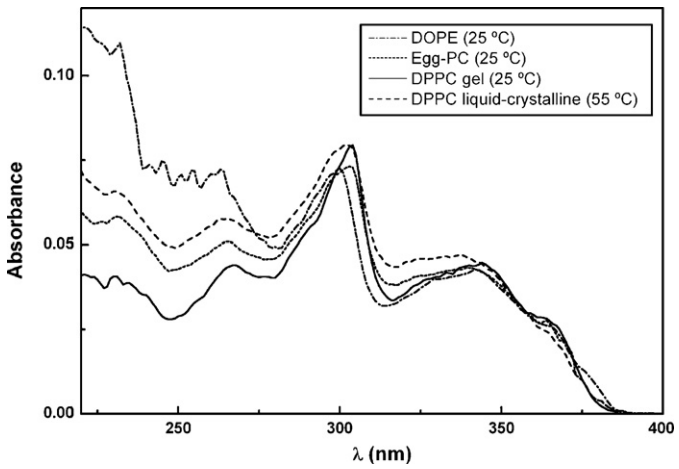

Fig. 7. Absorption spectra of **BTP** (2×10^{-6} M) in lipid membranes of DOPE, Egg-PC and DPPC at both gel (25 °C) and liquid-crystalline phases (55 °C).

Anisotropy and quantum yield values in ethylene glycol at room temperature were also determined for comparison.

Fluorescence quantum yields are roughly similar in all lipid bilayers and in ethylene glycol at 25 °C, with a small decrease in Egg-PC. The Strickler–Berg equation [36] relates the radiative lifetime with the absorption intensity (Eq. (6)):

$$\frac{1}{\tau_r} = 2.88 \times 10^{-9} n^2 \frac{\int F_{\bar{\nu}}(\bar{\nu}_F)\,d\bar{\nu}_F}{\int \bar{\nu}_F^{-3} F_{\bar{\nu}}(\bar{\nu}_F)\,d\bar{\nu}_F} \int \frac{\varepsilon(\bar{\nu}_A)\,d\bar{\nu}_A}{\bar{\nu}_A} \quad (6)$$

where τ_r is the radiative lifetime, n is the refraction index, ε is the molar extinction coefficient, and $F_{\bar{\nu}}(\bar{\nu}_F)$ is the fluorescence intensity per unit wave number, which is related to the fluorescence quantum yield [23] (Eq. (7)):

$$\int_{\infty}^{0} F_{\bar{\nu}}(\bar{\nu}_F)\,d\bar{\nu}_F = \Phi_F \quad (7)$$

Absorption spectra of **BTP** in the various lipid membranes at 25 °C (Fig. 7) are similar in the lowest energy absorption band. The Stickler–Berg relation (Eq. (6)) predicts an approximately constant value for the radiative lifetime in the three lipid membranes, considering the very small variations of the measured fluorescence quantum yields (Table 3).

The relation between the fluorescence quantum yield and the excited-state lifetime:

$$\Phi_F = k_r \tau \quad (8)$$

where $k_r = 1/\tau_r$ is the rate constant for radiative deactivation with fluorescence emission, allows the conclusion that the excited-state lifetimes are approximately constant for the studied lipid systems at 25 °C. Therefore, variations in fluorescence anisotropy values at this temperature can be directly related to changes in the rotational correlation time of the fluorophore and, thus, to changes in the microviscosity of the surrounding medium of the fluorescent molecule. It can be observed that r values in DPPC at gel phase (25 °C) and in Egg-PC are higher than the one obtained in ethylene glycol, indicating that **BTP** is deeply located in the lipid bilayer. The steady-state anisotropy in Egg-PC is higher than expected, comparing all anisotropy values in lipid bilayers at fluid phases (Egg-PC, DOPE and DPPC at 55 °C). A similar behaviour in Egg-PC was already observed for indole-2-carboxylate derivatives, prepared by us, substituted in the 3-position with either a dibenzothiophene or a dibenzofuran [37].

The phospholipid DOPE, at room temperature, adopts the inverse hexagonal phase, where the lipid molecules can adopt inverse curvature at the interface, allowing the chains to expand and at the same time reduce the head group area at the interface [38]. The very low anisotropy value observed in DOPE (Table 3) reflects the different geometry of self-organized DOPE aggregates, through the mentioned chain expansion. The emission spectrum (Fig. 6) shows that **BTP** feels a similar environment in DOPE to that in Egg-PC and DPPC at the liquid-crystalline phase.

In DPPC at 55 °C, a significant fluorescence quenching (Table 3) is observed due to the increase of the non-radiative deactivation pathways at higher temperatures. According to Eq. (5), an increase of the steady-state anisotropy is predicted from a decrease of the excited-state lifetime. **BTP** exhibits a significant decrease in anisotropy in DPPC at 55 °C (Table 3), showing that this molecule detects the phospholipid gel to liquid-crystalline phase transition and the associated decrease of microviscosity. The anisotropy value in the DPPC fluid phase is similar to the one in ethylene glycol at 25 °C, as observed in heteroaryl and heteroannulated indoles [37]. The results obtained in DPPC vesicles clearly indicate that **BTP** is located deeply in the lipid bilayer and that the red shift in emission at 55 °C may be due to the higher water penetration and not to a different localization of **BTP** in fluid phases.

Liposomes have been widely employed to deliver anticancer agents. Considering the **BTP** antitumoral activity and its preferential location near the phospholipid tails of lipid membranes, these studies are also important to drug delivery assays using liposomes.

4. Conclusions

The methyl 3-(benzo[*b*]thien-2-yl)benzothieno[3,2-*b*]pyrrole-2-carboxylate (**BTP**) interferes with the growth of different human tumour cell lines, exhibiting a stronger effect against the NCI-H460 lung cancer cell line.

This compound shows a solvent sensitive fluorescence emission and very reasonable fluorescence quantum yields (20–32%) in both polar and non-polar solvents. The estimated excited-state dipole moment (7.38 D) points to an ICT character of the excited state, confirmed by molecular quantum chemistry calculations.

Studies of incorporation in lipid bilayers revealed that **BTP** preferential location is near the hydrophobic lipid tails. Overall, these results point to a promising use of **BTP** as an antitumoral drug with the possibility of being transported in the hydrophobic region of liposomes.

Acknowledgements

We acknowledge the Foundation for the Science and Technology (FCT) – Portugal and FEDER (European Communitarian Fund) for financial support to Centro de Física and Centro de Química of Minho University, through the project PTDC/QUI/81238/2006. Computational facilities supported by FCT and University of Minho under project SeARCH (ref. REEQ/443/EEI/2005) are also acknowledged. A.S.A. acknowledges FCT for a post-doc. Grant SFRH/BPD/24548/2005.

References

[1] (a) B. Attenni, J.I.M. Hernando, S. Malancona, F. Narjes, J. M. Ontoria Ontoria, M. Rowley, Thienopyrroles as Antiviral Agents, Istituto di Ricerche di Biologia Molecolare P Angeletti S.p.A., Italy, WO/2005/023819, 2005.;
(b) S. Colarusso, J. Habermann, F. Narjes, S. Ponzi, M.R. Rico Ferreira, Thienopyrroles as Antiviral Agents, Istituto di Ricerche di Biologia Molecolare P Angeletti S.p.A., Italy, WO/2006/119975, 2006.
[2] B. Pelcman, K. Olofsson, P. Arsenjans, V. Ozola, E. Suna, I. Kalvins, Thienopyrroles Useful in the Treatment of Inflammation, Biolipox AB, Solna, SE, WO/2006/077412, 2006.
[3] D.W. Beight, J.M. Morin, Jr., J.S. Sawyer, E.C.R. Smith, Substituted Pyrrole Compounds and Their Use as sPLA2 Inhibitors, Eli Lilly & Co., Indianapolis, US, WO/2002/012249, 2002.
[4] A.J. Barker, J.G. Kettle, A.W. Faull, Indole Derivatives and Their Use as MCP-1 Antagonist, Zeneca Ltd., UK, WO/99/40914, 1999.

[5] A.M. Birch, A.D. Morley, A. Stocker, P.R.O. Whittamore, Heterocyclic Amide Derivatives as Inhibitors of Glycogen Phosphorylase, Astrazeneca AB, WO/2003/074532, 2003.
[6] J.C. Arnould, Thieno-pyrrole Compounds as Antagonists of Gonadotropin Releasing Hormone, Astrazeneca AB, WO/2004/018479, 2004.
[7] J.B. Blair, D. Marona-Lewicka, A. Kanthasamy, V.L. Lucaites, D.L. Nelson, D.E. Nichols, Thieno[3,2-*b*]- and thieno[2,3-*b*]pyrrole bioisosteric analogues of the hallucinogen and serotonin agonist *N*,*N*-dimethyltryptamine, J. Med. Chem. 42 (1999) 1106–1111.
[8] Y.-Q. Fang, J. Yuen, M. Lautens, A general modular method of azaindole and thienopyrrole synthesis *via* Pd-catalyzed tandem couplings of *gem*-dichloroolefins, J. Org. Chem. 72 (2007), 5152–5160 (and references cited therein).
[9] K.E. Chippendale, B. Iddon, H. Suschitzky, Condensed thiophene ring systems. Part X. Synthesis and reactions of 2-aryl-1H-[1]benzothieno[2,3-b]pyrroles and 2-aryl-1H-[1]benzothieno[3,2-b]pyrroles, J. Chem. Soc. Perkin I (1973) 125–129.
[10] A.S. Abreu, N.O. Silva, P.M.T. Ferreira, M.-J.R.P. Queiroz, M. Venanzi, New β,β-Bis(benzo[*b*]thienyl)dehydroalanine derivatives: synthesis and cyclization, Eur. J. Org. Chem. (2003) 4792–4796.
[11] R. Banerjee, Liposomes: applications in medicine, J. Biomater. Appl. 16 (2001) 3–21.
[12] B.R. Lentz, Membrane "fluidity" as detected by diphenylhexatriene probes, Chem. Phys. Lipids 50 (1989) 171–190.
[13] J.N. Demas, G.A. Crosby, The measurement of photoluminescence quantum yields. A review, J. Phys. Chem. 75 (1971) 991–1024.
[14] S. Fery-Forgues, D. Lavabre, Are fluorescence quantum yields so tricky to measure? A demonstration using familiar stationery products, J. Chem. Educ. 76 (1999) 1260–1264.
[15] J.V. Morris, M.A. Mahaney, J.R. Huber, Fluorescence quantum yield determinations. 9,10-Diphenylanthracene as a reference standard in different solvents, J. Phys. Chem. 80 (1976) 969–974.
[16] J.R. Lakowicz, Principles of Fluorescence Spectroscopy, 2nd edition, Kluwer Academic/Plenum Press, New York, 1999.
[17] N. Mataga, T. Kubota, Molecular Interactions and Electronic Spectra, Marcel Dekker, New York, 1970.
[18] P. Skehan, R. Storeng, D. Scudiero, A. Monks, J. McMahon, D. Vistica, J.T. Warren, H. Bokesch, S. Kenny, M.R. Boyd, New colorimetric cytotoxicity assay for anticancer-drug screening, J. Natl. Cancer Inst. 82 (1990) 1107–1112.
[19] A. Monks, D. Scudiero, P. Skehan, R. Shoemaker, K. Paul, D. Vistica, C. Hose, J. Langley, P. Cronise, A. Vaigro-Wolff, M. Gray-Goodrich, H. Campbell, J. Mayo, M. Boyd, Feasibility of a high-flux anticancer drug screen using a diverse panel of cultured human tumor cell lines, J. Natl. Cancer Inst. 83 (1991) 757–766.
[20] M.-J.R.P. Queiroz, A.S. Abreu, M.S.D. Carvalho, P.M.T. Ferreira, N. Nazareth, M.S.-J. Nascimento, Synthesis of new heteroaryl and heteroannulated indoles from dehydrophenylalanines: antitumor evaluation, Bioorg. Med. Chem. 16 (2008) 5584–5589.
[21] M.-J.R.P. Queiroz, R.C. Calhelha, L.A. Vale-Silva, E. Pinto, M.S.-J. Nascimento, Synthesis of novel 3-(aryl)benzothieno[2,3-*c*]pyran-1-ones from Sonogashira products and intramolecular cyclization: antitumoral activity evaluation, Eur. J. Med. Chem. 44 (2009) 1893–1899.
[22] C.A. Frederick, L.D. Williams, G. Ughetto, G.A. van der Marel, J.H. van Boom, A. Rich, A.H. Wang, Structural comparison of anticancer drug-DNA complexes: adriamycin and daunomycin, Biochemistry 29 (1990) 2538–2549.
[23] B. Valeur, Molecular Fluorescence—Principles and Applications, Wiley–VCH, Weinheim, 2002.
[24] N.J. Turro, Modern Molecular Photochemistry, Benjamin/Cummings Pub, Menlo Park, CA, 1978.
[25] M.-J.R.P. Queiroz, E.M.S. Castanheira, A.M.R. Pinto, I.C.F.R. Ferreira, A. Begouin, G. Kirsch, Synthesis of the first thieno-δ-carboline. Fluorescence studies in solution and in lipid vesicles, J. Photochem. Photobiol. A: Chem. 181 (2006) 290–296.
[26] M.-J.R.P. Queiroz, E.M.S. Castanheira, T.C.T. Lopes, Y.K. Cruz, G. Kirsch, Synthesis of fluorescent tetracyclic lactams by a "one pot" three steps palladium-catalyzed borylation, Suzuki coupling (BSC) and lactamization. DNA and polynucleotides binding studies, J. Photochem. Photobiol. A: Chem. 190 (2007) 45–52.
[27] D.R. Lide (Ed.), Handbook of Chemistry and Physics, 83rd edition, CRC Press, Boca Raton, 2002.
[28] (a) K.C. James, P.R. Noyce, Hydrogen bonding between testosterone propionate and solvent in chloroform-cyclohexane solutions, Spectrochim. Acta A 27 (1971) 691–696;
(b) G.R. Wileylb, S.I. Miller, Thermodynamic parameters for hydrogen bonding of chloroform with Lewis Bases in cyclohexane. A proton magnetic resonance study, J. Am. Chem. Soc. 94 (1972) 3287–3293.
[29] M.W. Schmidt, K.K. Baldridge, J.A. Boatz, S.T. Elbert, M.S. Gordon, J.H. Jensen, S. Koseki, N. Matsunaga, K.A. Nguyen, S. Su, T.L. Windus, M. Dupuis, J.A. Montgomery, General atomic and molecular electronic structure system, J. Comput. Chem. 14 (1993) 1347–1363.
[30] F. Jensen, Introduction to Computational Chemistry, John Wiley & Sons, West Sussex, England, 1999.
[31] Z.R. Grabowski, K. Rotkiewicz, W. Rettig, Structural changes accompanying intramolecular electron transfer; focus on TICT states and structures, Chem. Rev. 103 (2003) 3899–4031.
[32] M.-J.R.P. Queiroz, E.M.S. Castanheira, M.S.D. Carvalho, A.S. Abreu, P.M.T. Ferreira, H. Karadeniz, A. Erdem, New tetracyclic heteroaromatic compounds based on dehydroamino acids. Photophysical and electrochemical studies of interaction with DNA, Tetrahedron 64 (2008) 382–391.
[33] J.R. Silvius, Thermotropic phase transitions of pure lipids in model membranes and their modifications by membrane proteins, in: Lipid–Protein Interactions, John Wiley & Sons, New York, 1982.
[34] G.E.S. Toombes, A.C. Finnefrock, M.W. Tate, S.M. Gruner, Determination of L_α–H_{II} phase transition temperature for 1,2-dioleoyl-*sn*-glycero-3-phosphatidylethanolamine, Biophys. J. 82 (2002) 2504–2510.
[35] D. Papahadjopoulos, N. Miller, Phospholipid model membranes. I. Structural characteristics of hydrated liquid crystals, Biochim. Biophys. Acta 135 (1967) 624–638.
[36] S.J. Strickler, R.A. Berg, Relationship between absorption intensity and fluorescence lifetime of molecules, J. Chem. Phys. 37 (1962) 814.
[37] E.M.S. Castanheira, A.S. Abreu, M.S.D. Carvalho, M.-J.R.P. Queiroz, P.M.T. Ferreira, Fluorescence studies on potential antitumoral heteroaryl and heteroannulated indoles in solution and in lipid membranes, J. Fluorescence 19 (2009) 501–509.
[38] J.M. Seddon, Structure of the inverted hexagonal (H_{II}) phase and non-lamellar phase transitions in lipids, Biochim. Biophys. Acta 1031 (1990) 1–69.